Bioorganic Chemistry 111 (2021) 104832

Contents lists available at ScienceDirect

Bioorganic Chemistry

journal homepage: www.elsevier.com/locate/bioorg

Controlling the selectivity of aminergic GPCR ligands from the extracellular vestibule

Attila Egyed [a], Ádám A. Kelemen [a], Márton Vass [a,b], András Visegrády [c], Stephanie A. Thee [b], Zhiyong Wang [b], Chris de Graaf [d], Jose Brea [e], Maria Isabel Loza [e], Rob Leurs [b], György M. Keserű [a,*]

[a] Medicinal Chemistry Research Group, Research Center for Natural Sciences Magyar tudósok krt. 2, Budapest, H-1117, Hungary
[b] Division of Medicinal Chemistry, Faculty of Sciences, Amsterdam Institute for Molecules, Medicines and Systems (AIMMS), Vrije Universiteit Amsterdam, De Boelelaan 1108, Amsterdam, 1081 HZ, Netherlands
[c] Gedeon Richter plc. Gyömröi út 19-21, Budapest, H-1103, Hungary
[d] Sosei Heptares, Steinmetz Granta Park, Great Abington, Cambridge CB21 6DG, UK
[e] Innopharma Screening Platform, BioFarma Research Group, Center for Research in Molecular Medicine and Chronic Diseases (CIMUS), University of Santiago de Compostela, 15782, Santiago de Compostela, Spain

ARTICLE INFO

Keywords:
GPCR
Selectivity
Bitopic ligand
Secondary binding pocket
Fragment linking

ABSTRACT

In addition to the orthosteric binding pocket (OBP) of GPCRs, recent structural studies have revealed that there are several allosteric sites available for pharmacological intervention. The secondary binding pocket (SBP) of aminergic GPCRs is located in the extracellular vestibule of these receptors, and it has been suggested to be a potential selectivity pocket for bitopic ligands. Here, we applied a virtual screening protocol based on fragment docking to the SBP of the orthosteric ligand-receptor complex. This strategy was employed for a number of aminergic receptors. First, we designed dopamine D_3 preferring bitopic compounds from a D_2 selective orthosteric ligand. Next, we designed 5-HT_{2B} selective bitopic compounds starting from the 5-HT_{1B} preferring ergoline core of LSD. Comparing the serotonergic profiles of the new derivatives to that of LSD, we found that these derivatives became significantly biased towards the desired 5-HT_{2B} receptor target. Finally, addressing the known limitations of H_1 antihistamines, our protocol was successfully used to eliminate the well-known side effects related to the muscarinic M_1 activity of amitriptyline while preserving H_1 potency in some of the designed bitopic compounds. These applications highlight the usefulness of our new virtual screening protocol and offer a powerful strategy towards bitopic GPCR ligands with designed receptor profiles.

1. Introduction

G protein-coupled receptors (GPCRs) represent the largest protein family of drug targets, as 34% of FDA-approved drugs act on 108 GPCRs [1]. Although many of these medicines were designed to target a single receptor, it has been increasingly recognized that many drugs act on more than one target protein [2,3]. The first approach follows the "one drug, one target" paradigm and requires "magic bullet" compounds that are highly specific for the particular target. The multitarget approach needs ligands with optimally designed (or unintentionally discovered) receptor profiles, which has been recognized as a powerful strategy for central nervous system pharmacotherapy. Considering only aminergic GPCRs, 60% of the marketed drugs are "magic bullets", while 40% of the drugs target a specific combination of these receptors [4]. However, sequence and structural conservation of the 42 human aminergic GPCR subtypes makes the design principles less than obvious for both types of ligands.

Aminergic GPCRs recognize small biogenic amines such as acetylcholine, adrenaline, dopamine, histamine, and serotonin bound to an orthosteric site of the receptors. In addition to this evolutionarily conserved orthosteric binding pocket (OBP) formed by 7 transmembrane helices, recent structural studies have revealed the availability of another pocket located at the extracellular vestibule of aminergic GPCRs. This secondary binding pocket (SBP) may function as a stable or transient allosteric binding site (see Table S1 in the Supplementary Material for the definition of these binding pockets) [5]. For

* Corresponding author.
E-mail address: keseru.gyorgy@ttk.mta.hu (G.M. Keserű).

https://doi.org/10.1016/j.bioorg.2021.104832
Received 26 October 2020; Received in revised form 18 January 2021; Accepted 15 March 2021
Available online 19 March 2021

example, the muscarinic M_2 receptor harbours the allosteric modulator LY2119620 in the crystal structure of the ternary complex [6]. In the case of the β_2 adrenergic receptor, the SBP was transiently occupied during the simulation of the association/dissociation of the alprenolol ligand-receptor complex [7], and for the muscarinic M_3 receptor, tiotropium has been shown in simulations to bind to both binding sites [8].

Analysing the sequence and conformational similarity of both pockets, SBPs were found to be much less conserved than OBPs, supporting an SBP-focused strategy for designing ligands with specific receptor profiles for aminergic GPCRs [9] (see Fig. S2 in the Supplementary Material for the sequence comparison of the binding pockets of the receptors studied in this paper). Having developed bitopic compounds bound to both the OBP and the SBP, we and others have previously confirmed the role of the SBP in both the affinity and selectivity of these ligands [9–13]. Most of the promising bitopic compounds were, however, identified by trial and error, and the role of the different pockets was only confirmed retrospectively.

In this study, we present a prospective strategy for designing compounds for specific receptors using our multiple fragment docking protocol [10,14]. First, we docked suitable fragments into the OBP of the receptors and merged these fragments with the protein structure. Starting from the GPCR structure with a core fragment bound in the OBP, we performed a second round of virtual fragment screening against the SBP of the merged protein-ligand complex. The identified hit fragments in the SBP were then linked to the core OBP fragment, resulting in rationally designed bitopic ligands. These bitopic ligands were redocked to confirm the conserved binding modes of the OBP and SBP fragments. Finally, the designed bitopic compounds with the best fragment combinations were synthesized and tested experimentally. Using this new strategy, we were able to reverse the selectivity of the original OBP fragment for the dopaminergic D_2/D_3 and serotonergic 5-HT_{1B}/5-HT_{2B} receptor pairs and designed novel and selective H_1 antagonists free of off-target binding to the muscarinic M_1 receptor.

2. Results and discussion

2.1. Selectivity between the dopamine $D_{2/3}$ receptors

The first test of our design strategy was directed at the dopamine D_2 and D_3 receptor pair. The D_2 receptor has been established as an important target for atypical antipsychotics, including risperidone, and this drug has also been recently co-crystallized with the receptor [15]. This high-resolution X-ray structure confirmed that the tetrahydropyrido[1,2-*a*]pyrimidin-4-one ring of risperidone binds in the SBP, which differs considerably from that of the D_3 and D_4 receptors. Interestingly, however, risperidone does not show high D_2 selectivity over these receptor subtypes (K_i values are 2.4, 8.0 and 5.8 nM for D_2, D_3 and D_4, respectively [16]). In our work developing next-generation treatment options for mental diseases, we discovered cariprazine [17], a new drug approved by the US FDA and EMEA for psychosis, mania, and depression. Cariprazine shows a remarkable structural difference relative to all other marketed antipsychotics with a non-aromatic moiety in place of the previously indispensable aromatic pharmacophore in the SBP (Fig. 1). This feature also differentiates cariprazine from aripiprazole, another D_2 partial agonist that shares the identical 2,3-dichlorophenyl-piperazine core in the OBP. Comparing the dopamine receptor profile of cariprazine [18] to that of risperidone [19] and aripiprazole [18], cariprazine shows a clear preference towards the D_3 receptor. This has been proposed to account for the unprecedented efficacy of cariprazine on the negative symptoms of schizophrenia [20].

The correlation between the D_3 receptor preference and the unique pharmacophore of cariprazine prompted us to utilize our strategy to design novel bitopic ligands by fragment linking. In our previous study, we docked 266 aliphatic fragment candidates into the SBP in the presence of different core fragments bound to the OBP [10] (see all Computational Methods in the Supplementary Material). In the current

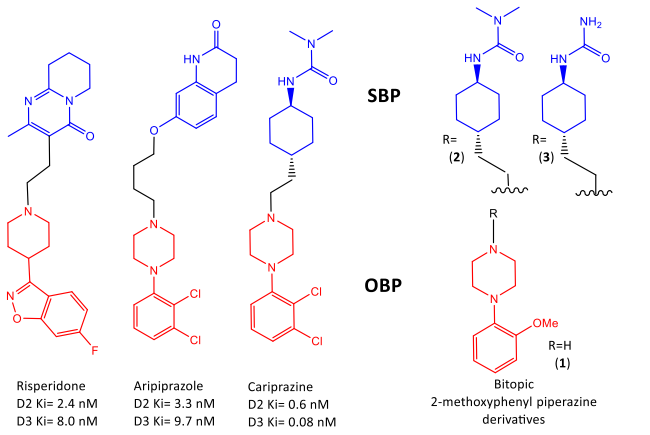

Fig. 1. Bitopic ligands identified to bind to the dopaminergic D_2 and D_3 receptors. OBP and SBP binder moieties are coloured red and blue, respectively. (For interpretation of the references to colour in this figure legend, the reader is referred to the web version of this article.)

work, starting from D_2 preferring 2-methoxyphenyl-piperazine core (**1**), we found that attaching the hit fragment *N*,*N*-dimethylcyclohexylurea from the virtual screening against the SBP of the D_3 receptor to the OBP core resulted in balanced D_2/D_3 bitopic compound **2**. Linking the cyclohexylurea fragment, which was the best scoring fragment for D_3, turned the OBP binder into D_3 preferring bitopic derivative **3** (Table 1). This observation has also been seen with other OBP cores [10] (see Fig. 5 for the proposed binding modes of **3**).

2.2. Selectivity between the serotonin 5-$HT_{1B/2B}$ receptors

Next, we challenged the design protocol against the serotonergic 5-HT_{1B} and 5-HT_{2B} receptors. We chose these targets since they represent another main group of aminergic GPCRs with multiple X-ray structures available. The first structures of both receptors were co-crystallized with the highly potent but non-selective antimigraine drug ergotamine [21,22]. Comparative analysis of the binding modes revealed that ergotamine binds to the orthosteric and secondary binding pockets. While the binding modes and the interaction patterns were very similar in the OBP, the binding modes in the corresponding SBPs were found to be significantly different (see Fig. S2 in the Supplementary Material and Fig. 5 for SBP comparison). First, the SBP available in the 5-HT_{1B} structure was expanded much more than the 5-HT_{2B} receptor. Furthermore, the bulky M218^{5x40} residue located in the SBP of the 5-HT_{2B} receptor is mutated to the much smaller T209^{5x40} in 5-HT_{1B}, which makes the 5-HT_{1B} SBP more accessible for larger ligands. More recently, the psychotropic ergoline derivative LSD has been co-crystallized with the 5-HT_{2B} receptor [23]. Although this crystal structure revealed slight binding mode differences, the ergoline ring system of ergotamine and LSD fit into the OBP in both cases. The ethyl groups of LSD do not reach the SBP and therefore LSD can be considered an OBP binder (Fig. 2).

Comparing the pharmacological profiles of these two compounds, LSD shows tenfold selectivity towards the 5-HT_{1B} receptor, activity that is absent for bitopic ergotamine, which has a balanced 5-HT_{1B}/5-HT_{2B}

Table 1
D_2 and D_3 receptor affinities of the OBP binding 2-methoxyphenyl-piperazine (**1**) and its bitopic derivatives (**2**, **3**). s.d. values are in parentheses.

SBP fragment	pK_i D_2	pK_i D_3	Selectivity
N/A (**1**)	6.17 (0.05)	5.65 (0.08)	D_2 preferred (ΔpK_i: −0.52)
N,*N*-dimethylcyclohexylurea (**2**)	8.67 (0.1)	8.79 (0.13)	Balanced D_2/D_3 (ΔpK_i: 0.12)
cyclohexylurea (**3**)	8.48 (0.1)	9.30 (0.15)	D_3 preferred (ΔpK_i: 0.82)

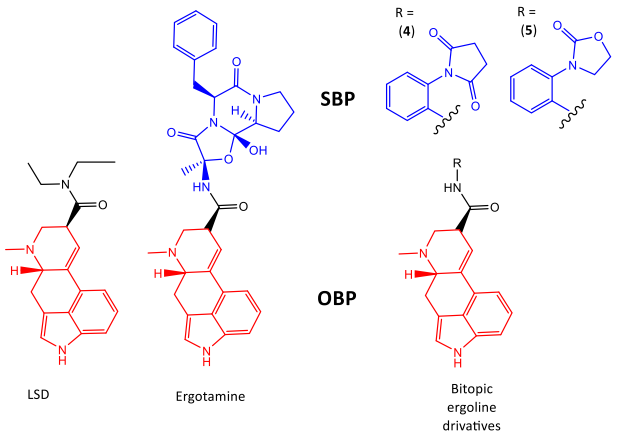

Fig. 2. Bitopic ligands identified to bind to the serotonergic 5-HT_{1B} and 5-HT_{2B} receptors. OBP and SBP binder moieties are coloured red and blue, respectively. (For interpretation of the references to colour in this figure legend, the reader is referred to the web version of this article.)

profile [24,25] (Table 2).

Our motivation again was to turn the selectivity of the OBP binding core in the opposite direction. Therefore, we applied our design protocol using a selected set of SBP fragments extracted from known bitopic 5-HT_{2B} binders available in the ChEMBL database [26] to improve selectivity towards the 5-HT_{2B} receptor. A set of 119 fragments was docked into the SBP of the 5-HT_{2B} receptor while keeping the ergoline core in the OBP. Linking the best-scored fragments to the OBP core through an amide bond, the resulting bitopic compounds were redocked, and conservation of the binding modes was confirmed in both the OBP and the SBP (see all Computational Methods in the Supplementary Material). The two best combinations were synthesized and tested for their 5-HT_{1B} and 5-HT_{2B} activity (Table 2). These results confirmed that linking carefully selected 5-HT_{2B} preferring SBP fragments to the unchanged OBP core enabled us to rationally design bitopic compounds **4** and **5** with the desired selectivity profiles, even achieving reversed selectivity relative to LSD, the starting OBP core. It is worth noting that the SBP fragment of **5** originates from the 5-HT_{1B}-selective compound CHEMBL1631542; however, in the docked binding poses of **5** and CHEMBL1631542, the SBP fragments are flipped and have different interactions with T/M^{5x40}, which are favourable for **5** and Y/T^{2x63} and F/L^{7x34}, which are favourable for CHEMBL1631542. This result highlights the potential of the proposed methodology to design bitopic ligands based on SBP virtual screening. Next, we investigated the impact of the designed SBP moieties on the broader aminergic receptor profile of the compounds and compared their profiles to those of LSD and ergotamine (Fig. 3).

This comparison revealed that ergotamine is more potent on the tested receptors than LSD and the less complex bitopic compounds. LSD, however, is more selective for serotonergic receptors, having much lower affinity towards adrenergic and dopaminergic receptors than ergotamine. The general serotonergic preference of LSD turned into a more specific 5-HT_{2B} preferring profile for the designed bitopic compounds. Compound **4** showed almost two orders of magnitude selectivity for 5-HT_{2B} over the other serotonin receptors, while compound **5** was active only on the 5-HT_{2B} and 5-HT_7 receptors, having a clear preference for the former (see Fig. 5 for the proposed binding modes of **5**).

Table 2
5-HT_{1B} and 5-HT_{2B} receptor affinities of OBP binding LSD and its bitopic derivatives (ergotamine, **4**, and **5**). s.d. values are in parentheses.

SBP fragment	pK_i 5-HT_{1B}	pK_i 5-HT_{2B}	Selectivity
N/A (LSD) [21]	8.50	7.50	5-HT_{1B} preferred (ΔpK_i: −1.00)
cyclic tripeptide (ergotamine) [22]	9.77	9.50	Balanced 5-$HT_{1B/2B}$ (ΔpK_i: −0.27)
1-(*o*-tolyl)pyrrolidine-2,5-dione (**4**)	6.12 (0.05)	7.24 (0.06)	5-HT_{2B} preferred (ΔpK_i: 1.12)
3-(*o*-tolyl)oxazolidin-2-one (**5**)	<5.00	6.79 (0.05)	5-HT_{2B} preferred (ΔpK_i: >1.79)

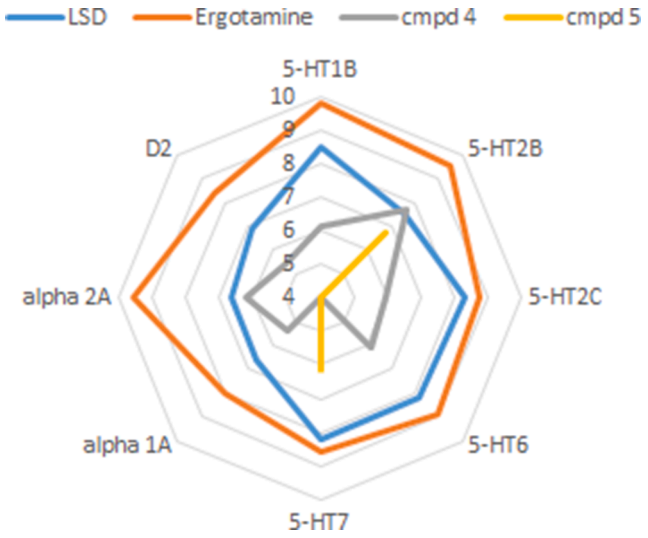

Fig. 3. Comparative receptor profile of LSD [24], ergotamine [25], and the designed bitopic compounds (**4** and **5**) measured against a panel of aminergic GPCRs. Binding affinities are expressed as pK_i values.

2.3. Selectivity between histamine H_1 and muscarinic acetylcholine M_1 receptors

Finally, we used the developed design protocol to address a therapeutic issue associated with first-generation antihistamines. These compounds were found to be fairly potent muscarinic acetylcholine M_1 receptor antagonists that cause reduced secretions in the airways and saliva [27] (Fig. 4).

Analysing the sequences and high-resolution crystal structures of the H_1 [28] and M_1 [29] receptors revealed that the corresponding OBPs are highly similar, but their SBPs are considerably different (see Fig. S2). Most of the key ligand-contacting residues are the same in the OBPs, with the most prominent change being the $F432^{6x52}$ to $N382^{6x52}$ mutation from H_1 to M_1, which introduces increased polarity and more specific interactions with the carbonyl group of acetylcholine in the muscarinic acetylcholine receptors. In contrast, the different sizes and

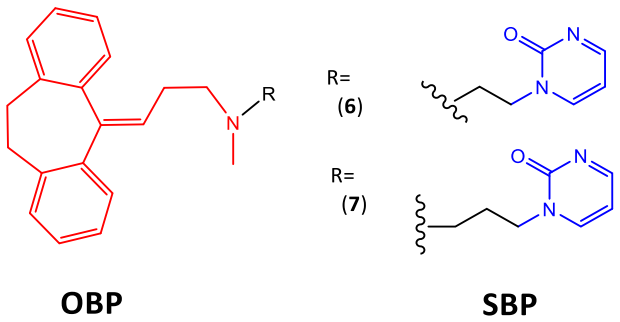

Fig. 4. Bitopic ligands identified to bind to the histamine H_1 and muscarinic acetylcholine M_1 receptors. OBP and SBP binding moieties are coloured red and blue, respectively. (For interpretation of the references to colour in this figure legend, the reader is referred to the web version of this article.)

characteristics of the SBPs suggest that connecting specific SBP fragments to the OBP binding core can improve H_1 selectivity. Considering the negatively charged character of the phosphate ion from the crystallization buffer found in the SBP in the X-ray structure of the H_1 receptor, we docked a library of commercial, in-house, and orthophosphate isostere fragments into this pocket in the presence of amitriptyline bound in the orthosteric pocket. We chose amitriptyline because this ligand binds only in the OBP, its histaminergic and muscarinergic profiles are largely known from the DrugMatrix database (literature pK_i values H_1: 9.3, H_2: 6.1, M_1: 8.6, M_2: 7.5, M_3: 8.3, M_4: 9.1, M_5: 8.2 [30]), and it is easy to derivatize starting from nortriptyline.

Linking the top scoring fragments through the basic amine group of the OBP core resulted in bitopic compounds that were redocked to investigate the conservation of the binding modes in the OBP and the SBP (see all Computational Methods in the Supplementary Material). The best SBP fragment, a pyrimidin-2-one unit, was linked to nortriptyline with either an ethyl (**6**) or propyl (**7**) linker and tested experimentally (Table 3). These results revealed that this design protocol is able to provide bitopic compounds with remarkable selectivity towards the preferred histamine H_1 target. Amitriptyline shows only 7-fold selectivity towards the H_1 receptor, whereas the designed bitopic compounds show 50- to 80-fold selectivity, with the propyl linker being the best option for high H_1 receptor affinity (Table 3) towards the desired target, proving to be useful candidates to study the relationship between selectivity and muscarinic receptor-related side effects (see Fig. 5 for the proposed binding modes of **7**).

It should be noted that high selectivities in this case may be attributable to the larger sequence and structural differences found between the H_1 and M_1 receptors, as they belong to different receptor families, compared to the available differences within a certain receptor family.

3. Conclusions

Targeting aminergic GPCRs requires precise selectivity or polypharmacological profiles for drug candidates to achieve the desired therapeutic effect. While an abundance of bitopic ligands are known for aminergic GPCRs, the complex receptor profiles of multitarget compounds could hardly be designed. Here, we present a general structure-based fragment linking methodology to exploit both the conservation of the orthosteric binding pocket (OBP) and the divergence of the secondary binding pocket (SBP) to design compounds with the desired affinity and selectivity profile against specific receptor pairs. We have demonstrated the utility of this virtual fragment screening and linking methodology to design compounds with different selectivity profiles against D_2/D_3, 5-HT_{1B}/5-HT_{2B}, and H_1/M_1 receptor pairs. We have shown that this general methodology is capable of delivering such compounds irrespective of the source of the fragments and the computational tools employed. The fragment and bitopic compound binding modes, binding pose robustness, and docking scores can also be used to rationalize the achieved selectivity. Although the computational and experimental data of the three case studies discussed in this work fully support the proposed design strategy of bitopic compounds, we should note that factors other than bitopic binding might also influence the selectivity observed. Available X-ray structures of the dopamine D_2 [15,33–35] and serotonin 5-HT_{2B} [22,23,36] receptors confirmed the effects of bitopic binding on selectivity. However, final proof would need X-ray studies with the present set of compounds. Since an increasing number of GPCR crystal structures have been elucidated, we envision that in the future, this method will be applicable not only to certain receptor pairs but also to design compounds with specific multi-receptor profiles, ultimately resulting in the desired on-target activity and reduced side effect profiles.

Table 3
H_1 and M_1 receptor affinities of OBP binding amitriptyline and its bitopic derivatives (**6** and **7**). s.d. values are in parentheses.

SBP fragment	pK_i H_1	pK_i M_1	Selectivity
N/A (amitriptyline)	9.20 (0.00)	8.32 (0.06)	H_1 preferred (ΔpK_i: 0.88)
1-ethylpyrimidin-2-one (**6**)	7.94 (0.03)	6.25 (0.15)	H_1 preferred (ΔpK_i: 1.69)
1-propylpyrimidin-2-one (**7**)	9.03 (0.06)	7.13 (0.07)	H_1 preferred (ΔpK_i: 1.90)

4. Experimental section

4.1. Computational Methods

The work on dopamine D_2-D_3 receptors has been addressed in Vass et al. [10] Briefly, the crystal structure of the D_3 receptor (PDB ID: 3PBL [37]) and a homology model of the D_2 receptor obtained using Schrödinger Prime 3.2 [38] were used for docking. A focused library of 196 fragments (comprising of a substituted aryl ring and a piperidine/piperazine moiety connected with a single bond or short linkers) were prepared with Schrödinger LigPrep 2.6 [38] and docked with Schrödinger Glide 5.9 [38] into the OBP of both receptors. Poses were filtered for H-bond interaction with D^{3x32}. The OBP fragments were then merged with the receptor structures in Maestro [38] and new docking grids were generated. A second focused fragment library of 266 substituted cyclohexyl amines and piperidines was docked into the SBP of the merged structures, and best fragment combinations based on docking scores were selected. Finally, the selected OBP and SBP fragments were linked with ethylene linkers and the resulting bitopic ligands were docked again in the apo structures of the receptors. In the present paper ligands were redocked into the crystal structure of the D_2 receptor (PDB ID: 6CM4 [15]) with Schrödinger Suite 2019-4 [39] using a similar protocol.

In case of the serotonin 5-HT_{1B}-5-HT_{2B} receptors a set of 119 virtual fragments was compiled by the fragmentation of known active and selective 5-HT_{1B} and 5-HT_{2B} ligands obtained from the ChEMBL 24 database [26]. The tripeptide moiety of ergotamine was cut off, and the remaining ergoline core was merged with the receptor structures resulting in four new receptor structures with the SBP as singular binding pocket. The fragment set was docked into the secondary binding pocket of these four merged receptor structures. The docking poses were filtered for occupying the SBP: based on the interactions with the non-conserved amino-acid pairs at 5-HT_{1B} and 5-HT_{2B} receptor SBP sites (Y/T^{2x63}, V/L^{45x52}, T/M^{5x40}, M/L^{6x58}, F/L^{7x34}) [9] and based on the principal interactions of the tripeptide moiety in the SBP. The two selected fragments (in compounds **4** and **5**) originated from the following compounds: ChEMBL1631542 (pK_i (5-HT_{1B}) = 8.7, pK_i (5-HT_{2B}) = 5.9) and ChEMBL1631544 (pK_i (5-HT_{1B}) = 7.4, 5-HT_{2B} data not available) respectively [40]. These best docked fragments were then linked to the ergoline scaffold by enumerating different regioisomers (*ortho, meta*, and *para* anilines) and $(CH_2)_{0\text{-}2}$ linkers between the aniline and the linker amide NH of ergotamine. All of the derivatives were docked into the original entire binding pocket of the four GPCR structures. Docked ligands were evaluated by Glide docking scores and poses were filtered by the criteria of H-bonding to D^{3x32}, occupation of the SBP cavity, and RMSD to the ergoline core.

The ligands were prepared for docking by generating possible ionization states (at a pH range of 7.0 ± 2.0), tautomers, and stereoisomers using Schrödinger's Ligand Preparation Wizard with default settings [41]. 2-2 X-ray structures of 5-HT_{1B} (PDB ID: 4IAQ, 4IAR [21]) and 5-HT_{2B} (PDB ID: 4IB4 [22], 4NC3 [36]) receptors were collected from the PDB database. The structures were first prepared for docking by keeping the monomeric receptor structure, removing crystallization agents (fatty acids, etc.) and using Schrödinger's Protein Preparation Wizard [41] with default settings, including the assignment of bond orders, adding missing side chains, and missing hydrogen atoms, creating disulphide bonds, removing crystalline waters, applying protomer-optimization, and restrained minimization with the OPLS_2005 force field.

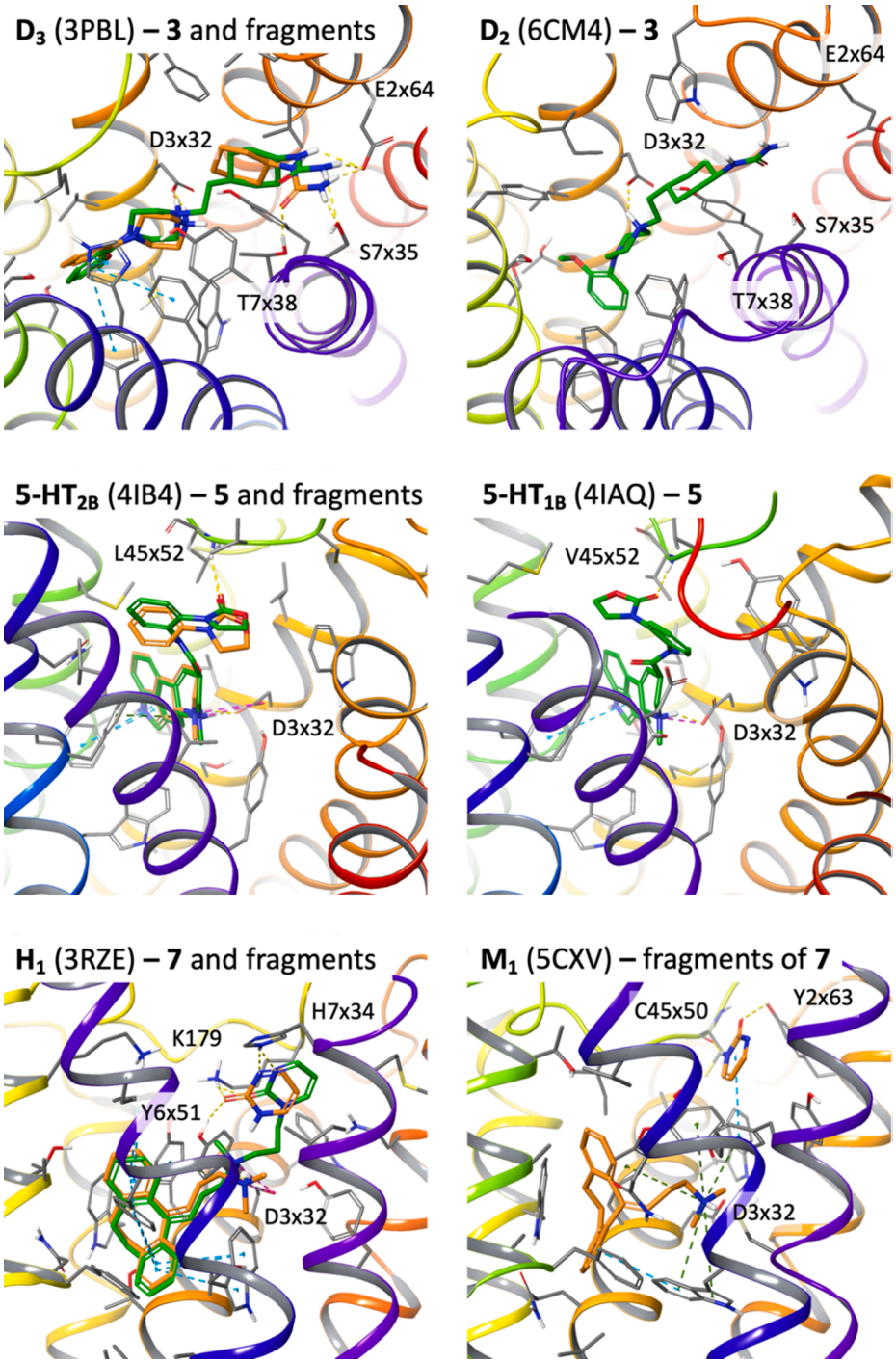

Fig. 5. Proposed binding modes of select bitopic compounds and their OBP and SBP fragments in the respective receptor structures. Compound **3** and its fragments 1-(2-methoxyphenyl)piperazine (OBP) and cyclohexylurea (SBP) bound in the dopamine D_3 receptor (PDB ID: 3PBL); **3** bound in the dopamine D_2 receptor (PDB ID: 6CM4); **4** and its fragments ergoline (OBP) and 1-phenylpyrrolidine-2,5-dione (SBP) bound in the serotonin 5-HT_{2B} receptor (PDB ID: 4IB4); **4** bound in the serotonin 5-HT_{1B} receptor (PDB ID: 4IAQ); **5** and its fragments ergoline (OBP) and 3-phenyl-1,3-oxazolidin-2-one (SBP) bound in the serotonin 5-HT_{2B} receptor (PDB ID: 4IB4); **5** bound in the serotonin 5-HT_{1B} receptor (PDB ID: 4IAQ); **7** and its fragments amitriptyline (OBP) and 2-pyrimidone (SBP) bound in the histamine H_1 receptor (PDB ID: 3RZE); these same fragments bound in the muscarinic acetylcholine M_1 receptor (PDB ID: 5CXV). Compound **7** could not be docked in the M_1 structure due to the closed tyrosine lid [31], and induced fit docking was not attempted. Docked binding modes were generated as outlined for each receptor in the Computational Methods section in the Supplementary Material. The OBP and SBP fragments are shown in thick orange, linked bitopic compounds are shown in thick green, protein residues within 3 Å of the ligands are shown in thin grey, the protein backbone is shown in rainbow ribbons from TM1-red to TM7-violet, H-bonds are shown as yellow dashes, aromatic stacking interactions are shown as blue dashes, ionic interactions are shown as pink dashes, and cation-pi interactions are shown as green dashes. Specific interacting residues in the SBP are shown with the GPCRdb structure-based numbering of each receptor [32]. (For interpretation of the references to colour in this figure legend, the reader is referred to the web version of this article.)

Structures were transformed into a receptor grid using Schrödinger software package, with the binding pocket centred on the D^{3x32} residue. All docking procedures have been conducted using Schrödinger's Glide software [41], with precision set to XP (Extra Precision).

In case of the histamine H_1 and muscarinic acetylcholine M_1 receptors OBP compounds were selected with available data from the ChEMBL 22 database [26]. Compounds were required to have PCHEMBL > 6 value available for the H_1 and $M_{1\text{-}5}$ receptors, and all within a 1.5 log unit interval. This was to ensure starting from active OBP ligands with a known selectivity profile, of which only four were found in the database (amitriptyline, benztropine, cyproheptadine, and orphenadrine). The ligands were protonated at pH 7.4 using ChemAxon cxcalc 5.1.4 [42] and 3D conformations were generated with Corina 3.59 [43] using the extra ring sampling option. The crystal structures of H_1 (PDB ID: 3RZE [28]) and M_1 (PDB ID: 5CXV [29]) were prepared with MOE 2015 [44]. Docking was performed with PLANTS [45] with IFP [46] post processing using the co-crystallized doxepin and tiotropium reference ligands. Standard settings were used for docking. The binding site was defined as the residues around the reference ligands with a radius of 6.5 Å. Poses were filtered for H-bond interaction with D^{3x32}. Docking poses were selected with the lowest PLANTS and highest IFP similarity scores as in de Graaf et al. 2011 [47]. The OBP fragments were then merged with the receptor structures in MOE.

The SBP fragment library was collected from several sources: i) the proprietary IOTA library with 1482 fragments, ii) the commercial MayBridge fragment screening library [48] with 2500 fragments, and

iii) orthophosphate bioisosteres from the PDB extracted with the protocol of Zhang et al. 2017 [49] adapted for the PDB ligand identifier "PO4" resulting in 393 additional fragments. The SBP fragments were prepared and docked using the same protocol as the OBP fragments, with the exception of the reference ligands used for IFP calculation. For H_1 the co-crystallized orthophosphate anion was used as the reference ligand. For M_1 the ligand CHEMBL2313377 was docked to the M_1 SBP using PLANTS, and the binding pose with the lowest RMSD of the maximum common substructure (MCS) with LY2119620 in the overlaid M_2 crystal structure (PDB ID: 4MQT [6]) was selected and used as a reference in further docking experiments. This was required as there are no co-crystallized M_1 allosteric modulators available in the PDB. CHEMBL2313377 is a known allosteric modulator of $M_{1,2,4}$ [50] of the same chemotype as LY2119620.

SBP fragment poses were filtered using a number of criteria. Since the binding sites and reference ligands for IFP were markedly different, the scores could not be directly compared, therefore poses in the top 16% (1σ in normal distribution) of the ligands ranked by both PLANTS score and IFP similarity were selected instead of defining a cut-off. The SBP fragment poses in the four OBP ligand merged structures had to show a robust docked binding pose within 1 Å RMSD of each other (calculated using fconv [51]). Fragments with the largest difference in average PLANTS score between H_1 and M_1 were then selected and linked to the four OBP ligands using $(CH_2)_{1\text{-}4}$ linkers at suitable synthetic handles (heteroatoms with a free H). The bitopic ligands were docked using the same protocol to the apo protein structures using the OBP compounds for IFP reference. Finally, the MCS RMSD was calculated between the SBP fragments and bitopic compounds using fconv [51], and only the fragments with <1 Å RMSD were kept.

4.2. Chemistry

4.2.1. Synthesis of dopamine D_2/D_3 ligands

The synthesis procedures of the dopamine D_2-D_3 receptor ligand have been reported in Vass et al. [10] The NMR experiments were performed at 500 MHz (^{1}H) on a Varian VNMR SYSTEM spectrometer. Chemical shifts are referenced to the residual solvent signals, 2.50 ppm for ^{1}H in DMSO-d_6. The LC-MS measurements were performed on Shimadzu LCMS2020 LC/MS system. Purifications by preparative-HPLC were performed with Hanbon NS4205 Binary high pressure semi-preparative HPLC. Thin-layer chromatography was performed on TLC Silica Gel 60 F^{254}. High resolution mass spectrometry measurements were performed using a Q-TOF Premier mass spectrometer (Waters Corporation, Milford, MA, USA) in positive electrospray ionization mode.

4.2.2. Synthesis of serotonin 5-HT_{1B}/5-HT_{2B} ligands

In case of the serotonin 5-HT_{1B}-5-HT_{2B} receptor ligands, procedures were based on Kobeissi et al. [52], Zhou et al. [53], and Cheung et al. [54] The NMR experiments were performed at 500 MHz (^{1}H) on a Varian VNMR SYSTEM spectrometer. Chemical shifts are referenced to the residual solvent signals, 2.50 ppm for ^{1}H in DMSO-d_6. The LC-MS measurements were performed on Shimadzu LCMS2020 LC/MS system. Purifications by preparative-HPLC were performed with Hanbon NS4205 Binary high pressure semi-preparative HPLC. Thin-layer chromatography was performed on TLC Silica Gel 60 F^{254}. High resolution mass spectrometry measurements were performed using a Q-TOF Premier mass spectrometer (Waters Corporation, Milford, MA, USA) in positive electrospray ionization mode.

4.2.2.1. 3,3-dimethyl-1-[(1R,4R)-4-{2-[4-(2-methoxyphenyl)piperazin-1-yl]ethyl}cyclohexyl]urea.

400 mg (1.26 mmol) (1r,4r)-4-{2-[4-(2-methoxyphenyl)piperazin-1-yl]ethyl}cyclohexan-1-amine was suspended in 50 mL of DCM. 695 µl (5 mmol) of TEA was added to the reaction mixture. Triphosgene (145 mg, 0.48 mmol) was dissolved in 5 mL of DCM and added dropwise to the previous mixture. The reaction mixture was stirred at room temperature for 1 h. In the next step, dimethylamine hydrochloride (410 mg, 5 mmol) and TEA (695 µl, 5 mmol) were added. The reaction was continued for 20 h at room temperature. The reaction mixture was filtered and the filtrate was washed with water. The phases were separated. The organic phase was dried over Na_2SO_4 and evaporated. The crude material was purified by flash chromatography, eluting with DCM: MeOH (0–5%). 160 mg (33%) white solid was obtained. ^{1}H NMR (500 MHz, DMSO-d_6) δ 7.05–6.96 (m, 2H), 6.96–6.87 (m, 2H), 3.79 (s, 3H), 3.53 (dd, J = 25.7, 12.3 Hz, 4H), 3.36 (tt, J = 11.5, 3.9 Hz, 1H), 3.24–3.06 (m, 4H), 3.00–2.86 (m, 2H), 2.75 (s, 6H), 1.75 (ddd, J = 24.4, 13.2, 3.6 Hz, 4H), 1.57 (dt, J = 11.6, 6.9 Hz, 2H), 1.21 (qd, J = 12.1, 3.1 Hz, 3H), 1.04–0.91 (m, 2H). ^{13}C NMR (125 MHz, DMSO-d_6) δ 157.49, 151.80, 139.25, 123.43, 120.77, 118.22, 116.78, 114.46, 111.90, 55.27, 53.84, 51.18, 51.11, 49.13, 46.98, 35.76, 34.38, 32.54, 31.41, 29.99. HRMS (ESI) $(M + H)^+$ calcd for $C_{22}H_{37}N_4O_2^+$, 389.2932; found 389.2939

4.2.2.2. 1-((1R,4R)-4-(2-(4-(2-methoxyphenyl)piperazin-1-yl)ethyl) cyclohexyl)urea.

400 mg (1.26 mmol) (1r,4r)-4-{2-[4-(2-methoxyphenyl)piperazin-1-yl]ethyl}cyclohexan-1-amine was suspended in 50 mL of DCM. 695 µl (5 mmol) of TEA was added to the reaction mixture. Triphosgene (145 mg, 0.48 mmol) was dissolved in 5 mL of DCM and added dropwise to the previous mixture. The reaction mixture was stirred at room temperature for 1 h. Subsequently, ammonia gas was introduced into the reaction mixture for 2 h. Thereafter, the reaction mixture was stirred at room temperature for 20 h. The reaction mixture was filtered and the filtrate was washed with water. The phases were separated. The organic phase was dried over Na_2SO_4 and evaporated. The crude material was purified by flash chromatography, eluting with DCM: MeOH (0–10%). 180 mg (40%) white solid was obtained. ^{1}H NMR (300 MHz, DMSO-d_6 + TFA-d_1) δ 10.04 (s, 1H), 7.11–6.83 (m, 4H), 3.80 (s, 3H), 3.54 (t, J = 15.1 Hz, 4H), 3.17 (s, 5H), 2.93 (t, J = 12.0 Hz, 2H), 1.77 (dd, J = 30.2, 10.8 Hz, 4H), 1.58 (dt, J = 11.7, 6.6 Hz, 2H), 1.24 (s, 1H), 1.03 (q, J = 12.9 Hz, 4H). ^{13}C NMR (75 MHz, DMSO-d_6 + TFA-d_1) δ 158.58, 152.32, 139.81, 123.96, 121.31, 118.74, 112.40, 55.82, 54.38, 51.66, 48.61, 47.52, 34.70, 33.35, 31.70, 30.45. HRMS (ESI) $(M + H)^+$ calcd for $C_{20}H_{33}N_4O_2^+$, 361.2603; found 361.2589.

4.2.2.3. (4R,7R)-N-[2-(2,5-dioxopyrrolidin-1-yl)phenyl]-6-methyl-6,11-diazatetracyclo[7.6.1.02,7.012,16]hexadeca-1(15),2,9,12(16),13-pentaene-4-carboxamide (S6)

To a mixture of *o*-nitroaniline (**S1**, 1380 mg, 10 mmol) and succinic acid (**S2**, 1180 mg, 10 mmol) polyphosphoric acid (PPA, 10 g) was added. The reaction mixture was stirred at 90 °C for 3 h. Afterwards the reaction was quenched by an ice:water mixture (10 g of ice in 20 mL of water) and the resulting crude 1-(2-nitrophenyl)pyrrolidine-2,5-dione (**S3**) was filtered of as a yellow precipitate. The crude product was dissolved in methanol:dimethyl-acetamide (3:1 mixture, 40 mL) in an autoclave and palladium on charcoal (10% Pd/C, 75 mg) was added to the solution. The reactor was filled with 5 bar of hydrogen gas, and the reaction mixture was stirred at room temperature overnight. The resulting suspension was filtered over Celite (30 g). To the filtrate was added water (50 mL) and the mixture was extracted with ethyl-acetate three times (15 mL × 3), and washed with sat. sodium-bicarbonate solution three times (10 mL × 3). To the collected organic phases was added hydrochloric acid (10% in water, 20 mL) and the aqueous phase was extracted with ethyl-acetate three times (15 mL × 3). The aqueous phase was made basic by the use of sodium-hydroxide solution (10% in water, 30 mL). The precipitate was filtered off and washed with water to afford the crude 1-(2-aminophenyl)pyrrolidine-2,5-dione (**S4**) as white crystals. To a solution of the crude 1-(2-aminophenyl)pyrrolidine-2,5-dione (**S4**) in dimethyl-formamide (10 mL) was added lysergic acid (**S5**, 134 mg, 0.5 mmol), HATU (209 mg, 0.55 mmol) and diisopropyl-ethylamine (DIPEA, 77 mg, 0.6 mmol, 0.104 mL). The reaction mixture was stirred overnight at room temperature, quenched by brine

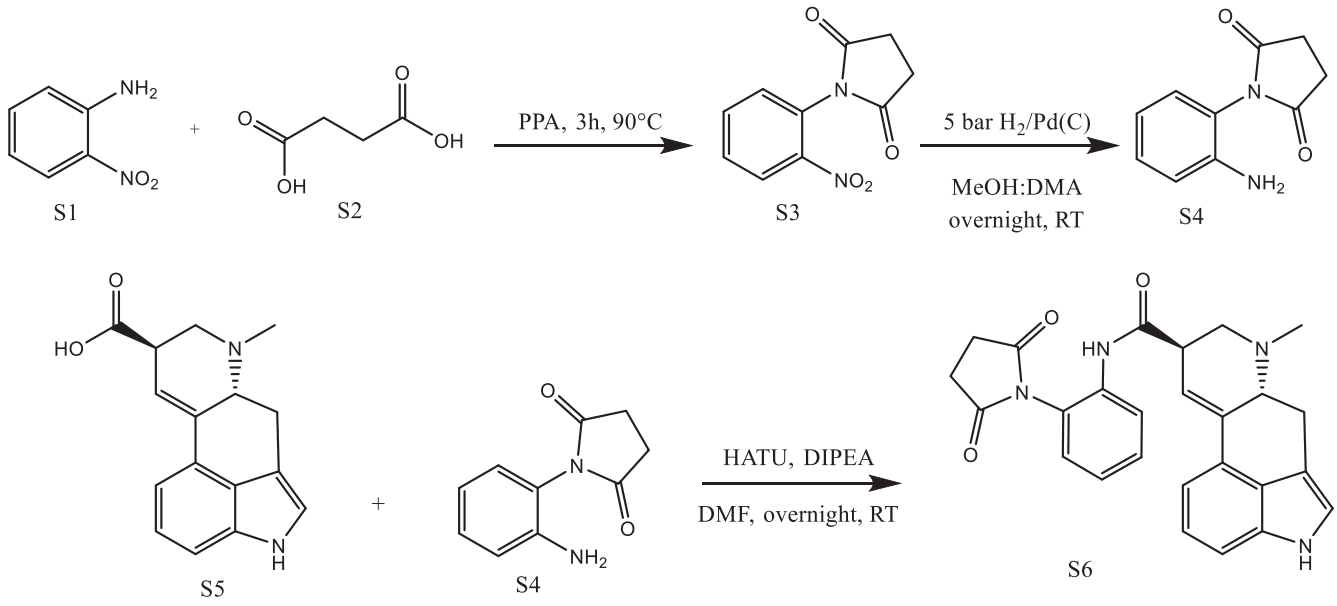

(20 mL) and extracted with ethyl acetate three times (10 mL × 3). The collected organic phases were evaporated under reduced pressure and the crude product was chromatographed in reverse phase preparative-HPLC (Eluent A: 0.1% formic acid in water; eluent B: 0.1% formic acid in acetonitrile; gradient: 0% to 100% B) to afford the title product (**S6**). Yield: 1.18 mg. ^{1}H NMR (500 MHz, DMSO-d_6) δ ppm 10.71 (s, 1H), 9.40 (s, 1H), 8.00 (d, J = 8.3 Hz, 1H), 7.39–7.36 (m, 1H), 7.21–7.16 (m, 3H), 7.11–7.05 (m, 3H), 6.51–6.50 (m, 1H), 4.28 (m, 1H), 3.55–3.51 (m, 1H), 3.44–3.40 (m, 1H), 3.20 (m, 2H), 3.14–3.07 (m, 2H), 2.71–2.61 (m, 3H), 2.51 (s, 3H). HR-MS (ESI +): *m/z* $[M + H]^+$ calcd. For $C_{26}H_{25}N_4O_3$: 441.1927; found: 441.1929.

4.2.2.4. (4R,7R)-6-methyl-N-[2-(2-oxo-1,3-oxazolidin-3-yl)phenyl]-6,11-diazatetracyclo[7.6.1.0^2,7.0^{12},^{16}]hexadeca-1(15),2,9,12(16),13-pentaene-4-carboxamide (S8)

To a solution of 3-(2-aminophenyl)-1,3-oxazolidin-2-one (**S7**, 107 mg, 0.6 mmol) in dimethyl-formamide (10 mL) was added lysergic acid (**S5**, 134 mg, 0.5 mmol), HATU (209 mg, 0.55 mmol) and DIPEA (77 mg, 0.6 mmol, 0.104 mL). The reaction mixture was stirred overnight at room temperature and was quenched by brine (20 mL). The mixture was extracted by ethyl-acetate three times (10 mL × 3). The collected organic phases were evaporated under reduced pressure and the crude product was chromatographed in reverse phase preparative-HPLC (Eluent A: 0.1% formic acid in water; eluent B: 0.1% formic acid in acetonitrile; gradient: 0% to 100% B) to afford the title product (**S8**). Yield: 1.03 mg. ^{1}H NMR (500 MHz, DMSO-d_6) δ ppm 10.70 (s, 1H), 10.08 (s, 1H), 8.16 (m, 1H), 7.40 (d, J = 7.66 Hz, 1H), 7.30 (t, J = 7.31 Hz, 1H), 7.23–7.17 (m, 1H), 7.13–7.05 (m, 4H), 6.57 (m, 1H), 4.49–4.36 (m, 3H), 4.02–3.93 (m, 2H), 3.88–3.83 (m, 1H), 3.58–3.54 (m, 1H), 3.19 (m, 2H), 3.08 (m, 1H), 2.58 (s, 3H). HR-MS (ESI +): *m/z* $[M + H]^+$ calcd. For $C_{25}H_{25}N_4O_3$: 429.1927; found: 429.1922

4.2.3. Synthesis of histamine H_1 /muscarinic acetylcholine M_1 receptor ligands

Anhydrous THF and DCM were obtained by elution through an activated alumina column prior to use. All other solvents and chemicals were acquired from commercial suppliers and were used as received. ChemBioDraw Ultra 16.0.1.4 was used to generate systematic names for all molecules. All reactions were performed under an inert atmosphere (N_2), unless mentioned otherwise. TLC analyses were carried out with alumina silica plates (Merck F_{254}) using staining and/or UV visualization. Column purifications were performed manually using Silicycle Ultra Pure silica gel or automatically using Biotage equipment. NMR spectra (^{1}H, ^{13}C, and 2D) were recorded on a Bruker 600 (600 MHz) spectrometer. Chemical shifts are reported in ppm (δ) and the residual solvent was used as internal standard. Data are reported as follows: chemical shift (integration, multiplicity (s = singlet, d = doublet, t = triplet, q = quartet, br = broad signal, m = multiplet, app = apparent), and coupling constants (Hz)). A Bruker microTOF mass spectrometer using ESI in positive ion mode was used to record HRMS spectra. A Shimadzu LC-20AD liquid chromatograph pump system linked to a Shimadzu SPD-M20A diode array detector with MS detection using a Shimadzu LC-MS-2010EV mass spectrometer was used to perform LC-MS analyses. An Xbridge (C18) 5 μm column (50 mm, 4.6 mm) was used. The solvents that were used were the following: solvent B (MeCN

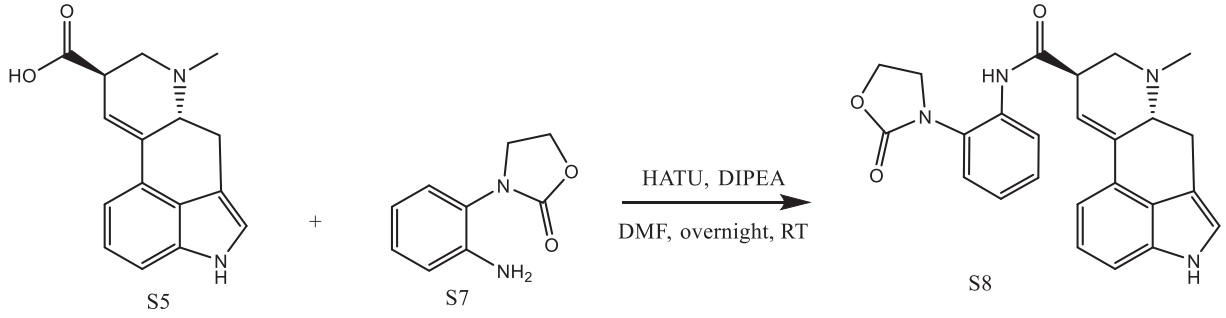

with 0.1% formic acid) and solvent A (water with 0.1% formic acid), flow rate of 1.0 mL/min, start 5% B, linear gradient to 90% B in 4.5 min, then 1.5 min at 90% B, then linear gradient to 5% B in 0.5 min, then 1.5 min at 5% B; total run time of 8 min. All final compounds have a purity of ≥95% (unless specified otherwise), calculated as the percentage peak area of the analyzed compound by UV detection at 254 nm (values are rounded).

4.2.3.1. 1-(2-((3-(10,11-dihydro-5H-dibenzo[a,d][7]annulen-5-ylidene) propyl)(methyl) amino)ethyl)pyrimidin-2(1H)-one (6, VUF16435)

The free base of nortriptyline hydrochloride (1.0 g, 3.3 mmol) was obtained using 2.5 M aq. NaOH (1.3 mL, 3.3 mmol). The resulting solution was extracted with DCM (3 × 30 mL). The collected organic phases were dried over Na_2SO_4, filtered and evaporated under reduced pressure. The crude product was dissolved in THF (20 mL). Et_3N (0.93 mL, 6.7 mmol) and 1,2-dibromoethane (0.57 mL, 6.7 mmol) were added. The reaction mixture was stirred for 12 d at RT. The resulting mixture was diluted with THF (20 mL). Et_3N (0.93 mL, 6.7 mmol) and pyrimidin-2(1H)-one hydrochloride (442 mg, 3.34 mmol) were added. The reaction mixture was stirred for 3 d at RT and diluted with water (30 mL). The mixture was extracted with EtOAc (3 × 30 mL). The collected organic phases were dried over Na_2SO_4, filtered and evaporated under reduced pressure. The crude product was purified using column chromatography (Eluent A: 2% Et_3N in cyclohexane; eluent B: 2% Et_3N in EtOAc; gradient: 20% to 80% B). Basic extraction with 2.5 M aq. NaOH and azeotropic distillation with EtOAc and hexane were performed to afford the title product as a colorless oil that solidifies over time. The compound retained EtOAc and hexane solvate even after extensive drying. Yield: 30 mg. ^{1}H NMR (600 MHz, $CDCl_3$) δ 8.42–8.34 (m, 1H), 7.59–7.47 (m, 1H), 7.23–7.11 (m, 6H), 7.07 (d, J = 7.4 Hz, 1H), 7.04 (d, J = 7.3 Hz, 1H), 5.84–5.76 (m, 1H), 5.71 (t, J = 7.3 Hz, 1H), 3.90 (app s, 2H), 3.35–3.23 (m, 2H), 3.00–2.90 (m, 1H), 2.79–2.67 (m, 3H), 2.49–2.40 (m, 2H), 2.24–2.19 (m, 2H), 2.15 (s, 3H). ^{13}C NMR (151 MHz, $CDCl_3$) δ 171.27, 165.85, 156.37, 149.28, 141.24, 139.94, 139.42, 137.14, 130.10, 129.24, 128.66, 128.38, 128.19, 127.64, 127.28, 126.18, 125.91, 103.25, 57.40, 55.48, 49.08, 41.62, 33.89, 32.17, 27.35. LC-MS (ESI): t_R = 3.53 min, purity: 98% (area % @ 254 nm), m/z $[M + H]^+$: 386. HR-MS (ESI +): m/z $[M + H]^+$ calcd. for $C_{25}H_{27}N_3O$: 386.2227; found: 386.2231.

4.2.3.2. 1-(3-((3-(10,11-dihydro-5H-dibenzo[a,d][7]annulen-5-ylidene)propyl)(methyl) amino)propyl)pyrimidin-2(1H)-one (7, VUF16412)

The free base of nortriptyline hydrochloride (1.0 g, 3.3 mmol) was obtained using 2.5 M aq. NaOH (1.3 mL, 3.3 mmol). The resulting solution was extracted with DCM (3 × 30 mL). The collected organic phases were dried over Na_2SO_4, filtered and evaporated under reduced pressure. The crude product was dissolved in THF (20 mL). Et_3N (1.4 mL, 10 mmol) and 1,3-dibromopropane (0.52 mL, 5.0 mmol) were added. The reaction mixture was stirred for 3 d at RT. To the resulting reaction mixture Et_3N (0.93 µl, 6.7 mmol) and pyrimidin-2(1H)-one hydrochloride (442 mg, 3.34 mmol) were added. The reaction mixture was stirred overnight at RT and another portion of pyrimidin-2(1H)-one hydrochloride (442 mg, 3.34 mmol) was added. The reaction mixture was stirred for 6 d at room temperature, diluted with water (30 mL) and extracted with EtOAc (3 × 50 mL). The collected organic phases were dried over Na_2SO_4, filtered and evaporated under reduced pressure. The crude product was purified using column chromatography twice (Eluent A: cyclohexane; eluent B: EtOAc; gradient: 10% to 100% B, followed by eluent A: DCM; eluent B: MeOH; gradient 3% to 5% B). Basic extraction with aq. 2.5 M NaOH was performed to afford the title product as a white solid. Yield: 160 mg. ^{1}H NMR (600 MHz, $CDCl_3$) δ 8.51 (dd, J = 4.1, 2.9 Hz, 1H), 7.64 (dd, J = 6.5, 2.9 Hz, 1H), 7.27 (dd, J = 4.9, 1.9 Hz, 1H), 7.23–7.10 (m, 6H), 7.07–7.01 (m, 1H), 6.03 (dd, J = 6.4, 4.1 Hz, 1H), 5.82 (app t, J = 7.3 Hz, 1H), 3.91 (br app s, 2H), 3.46–3.21 (m, 2H), 3.02–2.91 (br, 1H), 2.84–2.72 (br, 1H), 2.46–2.37 (m, 2H), 2.29 (app t, J = 7.3 Hz, 4H), 2.10 (s, 3H), 1.94 (app p, J = 6.6 Hz, 2H). ^{13}C NMR (151 MHz, $CDCl_3$) δ 165.90, 156.45, 149.10, 144.09, 141.20, 140.03, 139.44, 137.13, 130.21, 129.33, 128.57, 128.33, 128.23, 127.70, 127.33, 126.25, 125.92, 103.52, 57.31, 53.55, 49.93, 41.15, 33.87, 32.20, 27.28, 25.06. LC-MS (ESI): t_R = 3.49 min, purity: >99% (area % @ 254 nm), m/z $[M + H]^+$: 400. HR-MS (ESI +): m/z $[M + H]^+$ calcd. for $C_{26}H_{29}N_3O$: 400.2383, found: 400.2369.

4.3. Biological assays

4.3.1. Competition binding in human D_3 and D_2 receptors

For full experimental details see Vass et al. 2014 [10]. Briefly, membrane aliquots of CHO-K1 cells expressing human recombinant D_3 and D_2 receptors were thawed and washed in binding buffer and the assay was performed using tritiated raclopride at 25 °C for 120 min. Nonspecific binding was determined in the presence of excess haloperidol. At the end of incubation, samples were filtered on GF/B 96-well plates (Millipore) and washed four times with ice cold binding buffer. The plate was dried and 40 µl Microscint-20 scintillation cocktail was added to each well. Radioactivity was determined in a microplate beta scintillation counter (TopCount NXT, PerkinElmer, Waltham, MA, USA).

For dopamine D_2 receptor competition binding data shown on Fig. 3 experiments were carried out in a polypropylene 96-well plate. In each well was incubated 10 µg of membranes from CHO-D2 #S20 cell line prepared in our laboratory (Lot: A002/22-07-2015, protein concentration = 4185 µg/ml), 0.15 nM [^{3}H]-Spiperone (80.2 Ci/mmol, 1 mCi/ml, Perkin Elmer NET1187001MC) and compounds studied and standard. Non-specific binding was determined in the presence of Sulpiride 10 µM (Sigma S112). The reaction mixture (Vt: 250 µl/well) was incubated at 25 °C for 120 min, 200 µl was transferred to GF/C 96-well plate (Millipore, Madrid, Spain) pre-treated with 0.5% of PEI and treated with binding buffer (50 mM Tris-HCl,1 mM EDTA, 5 mM $MgCl_2$, 5 mM KCl, 120 mM NaCl, pH = 7.4), after was filtered and washed four times with 250 µl wash buffer (50 mM Tris-HCl, 0.9% NaCl, pH = 7.4), before measuring in a microplate beta scintillation counter (Microbeta Trilux, PerkinElmer, Madrid, Spain).

4.3.2. Competition binding for human 5-HT_{1B} receptor

Serotonin 5-HT_{1B} receptor competition binding experiments were carried out in a polypropylene 96-well plate. In each well was incubated 5 µg of membranes from Hela-5-HT1B cell line prepared in our laboratory (Lot: A001/14-11-2011, protein concentration = 3179 µg/ml), 1.5

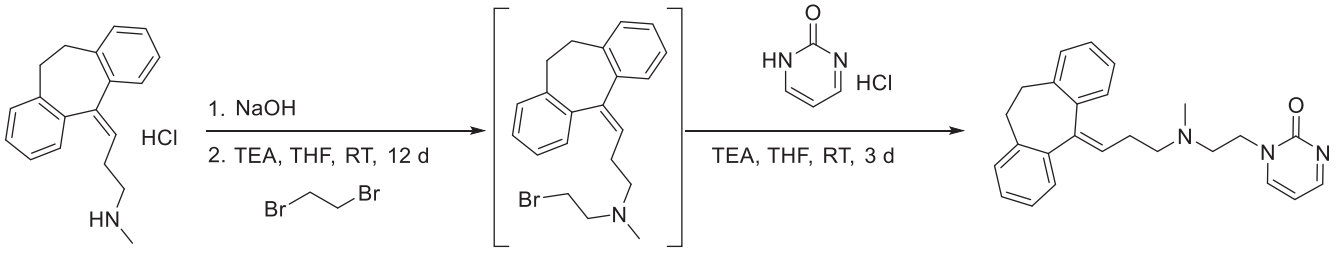

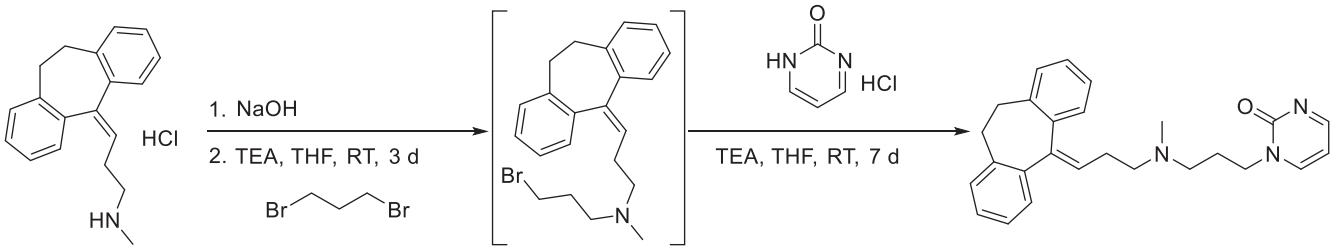

nM [^{3}H]-GR125743 (83.9 Ci/mmol, 0.1 mCi/ml, Perkin Elmer NET1172100UC) and compounds studied and standard. Non-specific binding was determined in the presence of GR55562 10 μM (TOCRIS 1054). The reaction mixture (Vt: 250 μl/well) was incubated at 25 °C for 90 min, 200 μl was transferred to GF/C 96-well plate (Millipore, Madrid, Spain) pre-treated with 0.5% of PEI and treated with binding buffer (Tris-HCl 50 mM, EDTA 1 mM, $MgCl_2$ 10 mM, pH = 7.4), after was filtered and washed four times with 250 μl wash buffer (Tris-HCl 50 mM, pH = 7.4), before measuring in a microplate beta scintillation counter (Microbeta Trilux, PerkinElmer, Madrid, Spain).

4.3.3. Competition binding for human 5-HT$_{2B}$ receptor

Serotonin 5-HT$_{2B}$ receptor competition binding experiments were carried out in a polypropylene 96-well plate. In each well was incubated 20 μg of membranes from CHO-5-HT2B cell line prepared in our laboratory (Lot: A004/19-10-2017, protein concentration = 2775 μg/ml), 0.8 nM [^{3}H]-LSD (82.9 Ci/mmol, 1 mCi/ml, Perkin Elmer NET638250UC) and compounds studied and standard. Non-specific binding was determined in the presence of 5-HT 50 μM (Sigma H9523). The reaction mixture (Vt: 250 μl/well) was incubated at 37 °C for 30 min, 200 μl was transferred to GF/C 96-well plate (Millipore, Madrid, Spain) pre-treated with 0.5% of PEI and treated with binding buffer (Tris-HCl 50 mM, Ascorbic acid 0.1%, $CaCl_2$ 4 mM, pH = 7.4), after was filtered and washed four times with 250 μl wash buffer (Tris-HCl 50 mM, pH = 7.4), before measuring in a microplate beta scintillation counter (Microbeta Trilux, PerkinElmer, Madrid, Spain).

4.3.4. Competition binding for human 5-HT$_{2C}$ receptor

Serotonin 5-HT$_{2C}$ receptor competition binding experiments were carried out in a polypropylene 96-well plate. In each well was incubated 3 μg of membranes from Hela-5-HT2C cell line prepared in our laboratory (Lot: A002/20-06-2011, protein concentration = 2041 μg/ml), 1.25 nM [^{3}H]-Mesulergine (84.7 Ci/mmol, 1 mCi/ml, Perkin Elmer NET1148250UC) and compounds studied and standard. Non-specific binding was determined in the presence of Mianserin 10 μM (Sigma M2525). The reaction mixture (Vt: 250 μl/well) was incubated at 27 °C for 60 min, 200 μl was transferred to GF/C 96-well plate (Millipore, Madrid, Spain) pre-treated with 0.5% of PEI and treated with binding buffer (50 mM Tris-HCl, pH = 7.5), after was filtered and washed four times with 250 μl wash buffer (50 mM Tris-HCl , pH = 6.6), before measuring in a microplate beta scintillation counter (Microbeta Trilux, PerkinElmer, Madrid, Spain).

4.3.5. Competition binding for human 5-HT$_6$ receptor

Serotonin 5-HT$_6$ receptor competition binding experiments were carried out in a polypropylene 96-well plate. In each well was incubated 5 μg of membranes from HEK-5-HT6#10p cell line prepared in our laboratory (Lot: A001/02-03-2010, protein concentration = 2624 μg/ml), 2 nM [^{3}H]-LSD (82.9 Ci/mmol, 1 mCi/ml, Perkin Elmer NET638250UC) and compounds studied and standard. Non-specific binding was determined in the presence of 5-HT 100 μM (Sigma H9523). The reaction mixture (Vt: 250 μl/well) was incubated at 37 °C for 60 min, 200 μl was transferred to GF/C 96-well plate (Millipore, Madrid, Spain) pre-treated with 0.5% of PEI and treated with binding buffer (50 mM Tris-HCl, 10 mM $MgCl_2$, 0.5 mM EDTA, pH = 7.4), after was filtered and washed four times with 250 μl wash buffer (50 mM Tris-HCl, pH = 7.4), before measuring in a microplate beta scintillation counter (Microbeta Trilux, PerkinElmer, Madrid, Spain).

4.3.6. Competition binding for human 5-HT$_7$ receptor

Serotonin 5-HT$_7$ receptor competition binding experiments were carried out in a polypropylene 96-well plate. In each well was incubated 2 μg of membranes from HEK-5-HT7#14 cell line prepared in our laboratory (Lot: A006/21-07-2016, protein concentration = 3316 μg/ml), 2 nM [^{3}H]-SB269970 (34.5 Ci/mmol, 0.25 mCi/ml, Perkin Elmer NET1198U250UC) and compounds studied and standard. Non-specific binding was determined in the presence of clozapine 25 μM (Sigma C6305). The reaction mixture (Vt: 250 μl/well) was incubated at 37 °C for 60 min, 200 μl was transferred to GF/C 96-well plate (Millipore, Madrid, Spain) pre-treated with 0.5% of PEI and treated with binding buffer (50 mM Tris-HCl, 4 mM $CaCl_2$, 1 mM ascorbic acid, 0.1 mM pargyline, pH = 7.4), after was filtered and washed four times with 250 μl wash buffer (50 mM Tris-HCl, 4 mM $CaCl_2$, 1 mM ascorbic acid, 0.1 mM pargyline, pH = 7.4) before measuring in a microplate beta scintillation counter (Microbeta Trilux, PerkinElmer, Madrid, Spain).

4.3.7. Competition binding for human α_{1A} adrenergic receptor

α_{1A} adrenergic receptor competition binding experiments were carried out in a polypropylene 96-well plate. In each well was incubated 20 μg of membranes from HEK-α1A#5 cell line prepared in our laboratory (Lot: A004/07-06-2017, protein concentration = 4171 μg/ml), 0.4 nM [^{3}H]-Prazosin (80.6 Ci/mmol, 1 mCi/ml, Perkin Elmer NET823250UC) and compounds studied and standard. Non-specific binding was determined in the presence of prazosin 1 μM (Sigma P115). The reaction mixture (Vt: 250 μl/well) was incubated at 25 °C for 90 min, 200 μl was transferred to GF/C 96-well plate (Millipore, Madrid, Spain) pre-treated with 0.5% of PEI and treated with binding buffer (50 mM Hepes, 5 mM $MgCl_2$, 1 mM $CaCl_2$, 0.2% BSA, pH = 7.4), after was filtered and washed four times with 250 μl wash buffer (50 mM Hepes, 500 mM NaCl, 0.1% BSA, pH = 7.4) before measuring in a microplate beta scintillation counter (Microbeta Trilux, PerkinElmer, Madrid, Spain).

4.3.8. Competition binding for human α_{2A} adrenergic receptor

α_{2A} adrenergic receptor competition binding experiments were carried out in a multiscreen GF/C 96-well plate (Millipore, Madrid, Spain) pre-treated with binding buffer (25 mM NaH_2PO_4 pH = 7.4). In each well was incubated 30 μg of membranes from CHO-α2A cell line prepared in our laboratory (Lot: A001/21-07-2009, protein concentration = 3330 μg/ml), 0.37 nM [^{3}H]-MK912 (87.5 Ci/mmol, 1 mCi/ml, Perkin Elmer NET1227250UC) and compounds studied and standard. Non-specific binding was determined in the presence of norepinephrine 100 μM (Sigma A7257). The reaction mixture (Vt: 200 μl/well) was incubated at 25 °C for 30 min after was filtered and washed four times with 250 μl wash buffer (25 mM NaH_2PO_4 pH = 7.4), before measuring in a microplate beta scintillation counter (Microbeta Trilux, PerkinElmer, Madrid, Spain).

4.3.9. Competition binding for human H_1 receptors

Histamine H_1 receptor competition binding experiments [55] were carried out in 96-multiwell plates (Greiner Bio-one, art. 655101). In each well was incubated; 25 µl compound (dissolved to the desired concentration in H_1R binding buffer (a 4:1 mix of 50 mM Na_2HPO_4 and 50 mM KH_2PO_4, pH 7.4) and 4% DMSO (Sigma Aldrich, art. 276855), 25 µl [^{3}H]-Pyrilamine (PerkinElmer, art. NET594250UC) diluted to 10 nM concentration in H_1R binding buffer and 50 µl of cell homogenate prepared from HEK293T cells (ATCC, Manassas, VA, USA) expressing the H_1 receptor as previously reported (Bosma et al., 2016). The reaction mixture was incubated for 60 min at 25 °C and 600 rpm. The reaction mixture was then harvested onto a GF/C 96-well plate (PerkinElmer, art. 6005174) pre-treated with 0.5% of PEI (Sigma-Aldrich, art. P3143). The GF/C plate was then washed three times with cold (4 °C) wash buffer (50 mM Tris, pH 7.4) and allowed to dry at 50 °C for 1 h. Once dry, 20 µl of scintillation fluid (PerkinElmer, art. 6013611) was added to each well, the plate sealed (PerkinElmer, art. 6050185) and measured in a microplate beta scintillation counter (Wallac Trilux, PerkinElmer).

4.3.10. Competition binding for human M_1 receptors

Muscarinic M_1 receptor competition binding experiments were carried out in a polypropylene 96-well plate. In each well was incubated 10 µg of membranes from M_1 cell line (Millipore, HTS044M, protein concentration = 2000 µg/ml), 2 nM [^{3}H]-Pirenzepine (85 Ci/mmol, 1 mCi/ml, Perkin Elmer NET780250UC) and compounds studied and standard. Non-specific binding was determined in the presence of Pirenzepine 200 µM (Sigma P7412). The reaction mixture (Vt: 250 µl/well) was incubated at 25 °C for 90 min, 200 µl was transferred to GF/C 96-well plate (Millipore, Madrid, Spain) pre-treated with 0.5% of PEI and treated with binding buffer (Hepes 50 mM, $MgCl_2$ 5 mM, $CaCl_2$ 1 mM, BSA 0.2%, pH = 7.4), after was filtered and washed four times with 250 µl wash buffer (Hepes 50 mM, NaCl 500 mM, BSA 0.1%, pH = 7.4), before measuring in a microplate beta scintillation counter (Microbeta Trilux, PerkinElmer, Madrid, Spain).

Declaration of Competing Interest

The authors declare that they have no known competing financial interests or personal relationships that could have appeared to influence the work reported in this paper.

Acknowledgements

The authors are grateful for the constructive discussions with Maikel Wijtmans and Iwan de Esch. This work has been supported by the National Brain Research Program (2017-1.2.1-NKP-2017-00002) to GMK and The Netherlands Organization for Scientific Research (NWO) TOP-PUNT ("7 ways to 7TMR modulation (7-to-7)"Grant 718.014.002) to RL.

The experimental assistance of Dr Tiffany van der Meer in some of the binding experiments is highly appreciated. Pál Szabó (RCNS) and Hans Custers (VUA) are acknowledged for HRMS measurements. Ruben Dekker and George Abdel Malek are acknowledged for their contributions to the H_1/M_1 computational procedures.

Appendix A. Supplementary data

Supplementary data to this article can be found online at https://doi.org/10.1016/j.bioorg.2021.104832.

References

[1] R. Santos, O. Ursu, A. Gaulton, A.P. Bento, R.S. Donadi, C.G. Bologa, A. Karlsson, B. Al-Lazikani, A. Hersey, T.I. Oprea, J.P. Overington, A comprehensive map of molecular drug targets, Nat. Rev. Drug Discov. 16 (2016) 19–34, https://doi.org/10.1038/nrd.2016.230.

[2] R. Chaudhari, Z. Tan, B. Huang, S. Zhang, Computational polypharmacology: a new paradigm for drug discovery, Expert Opin. Drug Discov. 12 (2017) 279–291, https://doi.org/10.1080/17460441.2017.1280024.

[3] E. Proschak, H. Stark, D. Merk, Polypharmacology by Design: A Medicinal Chemist's Perspective on Multitargeting Compounds, J. Med. Chem. 62 (2019) 420–444, https://doi.org/10.1021/acs.jmedchem.8b00760.

[4] A.S. Hauser, M.M. Attwood, M. Rask-Andersen, H.B. Schiöth, D.E. Gloriam, Trends in GPCR drug discovery: New agents, targets and indications, Nat. Rev. Drug Discov. 16 (2017) 829–842, https://doi.org/10.1038/nrd.2017.178.

[5] M. Vass, S. Podlewska, I.J.P. De Esch, A.J. Bojarski, R. Leurs, A.J. Kooistra, C. De Graaf, Aminergic GPCR-Ligand Interactions: A Chemical and Structural Map of Receptor Mutation Data, J. Med. Chem. 62 (2019) 3784–3839, https://doi.org/10.1021/acs.jmedchem.8b00836.

[6] A.C. Kruse, A.M. Ring, A. Manglik, J. Hu, K. Hu, K. Eitel, H. Hübner, E. Pardon, C. Valant, P.M. Sexton, A. Christopoulos, C.C. Felder, P. Gmeiner, J. Steyaert, W. I. Weis, K.C. Garcia, J. Wess, B.K. Kobilka, Activation and allosteric modulation of a muscarinic acetylcholine receptor, Nature 504 (2013) 101–106, https://doi.org/10.1038/nature12735.

[7] R.O. Dror, A.C. Pan, D.H. Arlow, D.W. Borhani, P. Maragakis, Y. Shan, H. Xu, D. E. Shaw, Pathway and mechanism of drug binding to G-protein-coupled receptors, Proc. Natl. Acad. Sci. USA 108 (2011) 13118–13123, https://doi.org/10.1073/pnas.1104614108.

[8] L.E.M. Kistemaker, C.R.S. Elzinga, C.S. Tautermann, M.P. Pieper, D. Seeliger, S. Alikhil, M. Schmidt, H. Meurs, R. Gosens, Second M3 muscarinic receptor binding site contributes to bronchoprotection by tiotropium, Br. J. Pharmacol. 176 (2019) 2864–2876, https://doi.org/10.1111/bph.14707.

[9] M. Michino, T. Beuming, P. Donthamsetti, A.H. Newman, J.A. Javitch, L. Shi, What can crystal structures of aminergic receptors tell us about designing subtype-selective ligands? Pharmacol. Rev. 67 (2015) 198–213, https://doi.org/10.1124/pr.114.009944.

[10] M. Vass, E. Agai-Csongor, F. Horti, G.M. Keserű, Multiple fragment docking and linking in primary and secondary pockets of dopamine receptors, ACS Med. Chem. Lett. 5 (2014) 1010–1014, https://doi.org/10.1021/ml500201u.

[11] G. Mattedi, F. Deflorian, J.S. Mason, C. De Graaf, F.L. Gervasio, Understanding Ligand Binding Selectivity in a Prototypical GPCR Family, J. Chem. Inf. Model. 59 (2019) 2830–2836, https://doi.org/10.1021/acs.jcim.9b00298.

[12] A.H. Newman, T. Beuming, A.K. Banala, P. Donthamsetti, K. Pongetti, A. Labounty, B. Levy, J. Cao, M. Michino, R.R. Luedtke, J.A. Javitch, L. Shi, Molecular determinants of selectivity and efficacy at the dopamine D3 receptor, J. Med. Chem. 55 (2012) 6689–6699, https://doi.org/10.1021/jm300482h.

[13] J.R. Lane, P.M. Sexton, A. Christopoulos, Bridging the gap: Bitopic ligands of G-protein-coupled receptors, Trends Pharmacol. Sci. 34 (2013) 59–66, https://doi.org/10.1016/j.tips.2012.10.003.

[14] M. Vass, Á. Tarcsay, G.M. Keseru, Multiple ligand docking by Glide: Implications for virtual second-site screening, J. Comput. Aided Mol. Des. 26 (2012) 821–834, https://doi.org/10.1007/s10822-012-9578-6.

[15] S. Wang, T. Che, A. Levit, B.K. Shoichet, D. Wacker, B.L. Roth, Structure of the D2 dopamine receptor bound to the atypical antipsychotic drug risperidone, Nature 555 (2018) 269–273, https://doi.org/10.1038/nature25758.

[16] J.A. Gray, B.L. Roth, The pipeline and future of drug development in schizophrenia, Mol. Psychiatry 12 (2007) 904–922, https://doi.org/10.1038/sj.mp.4002062.

[17] É. Ágai-Csongor, G. Domány, K. Nógrádi, J. Galambos, I. Vágó, G.M. Keser, I. Greiner, I. Laszlovszky, A. Gere, É. Schmidt, B. Kiss, M. Vastag, K. Tihanyi, K. Sághy, J. Laszy, I. Gyertyán, M. Zájer-Balázs, L. Gémesi, M. Kapás, Z. Szombathelyi, Discovery of cariprazine (RGH-188): A novel antipsychotic acting on dopamine D 3/D 2 receptors, Bioorganic Med. Chem. Lett. 22 (2012) 3437–3440, https://doi.org/10.1016/j.bmcl.2012.03.104.

[18] B. Kiss, A. Horváth, Z. Némethy, É. Schmidt, I. Laszlovszky, G. Bugovics, K. Fazekas, K. Hornok, S. Orosz, I. Gyertyán, É. Ágai-Csongor, G. Domány, K. Tihanyi, N. Adham, Z. Szombathelyi, Cariprazine (RGH-188), a dopamine D3 receptor-preferring, D 3/D2 dopamine receptor antagonist-partial agonist antipsychotic candidate: In vitro and neurochemical profile, J. Pharmacol. Exp. Ther. 333 (2010) 328–340, https://doi.org/10.1124/jpet.109.160432.

[19] J.S. Silvestre, J. Prous, Research on adverse drug events. I. Muscarinic M3 receptor binding affinity could predict the risk of antipsychotics to induce type 2 diabetes, Methods Find. Exp. Clin. Pharmacol. 27 (2005) 289–304, https://doi.org/10.1358/mf.2005.27.5.908643.

[20] S. Galderisi, A. Mucci, R.W. Buchanan, C. Arango, Negative symptoms of schizophrenia: new developments and unanswered research questions, Lancet Psychiatry 5 (2018) 664–677, https://doi.org/10.1016/S2215-0366(18)30050-6.

[21] C. Wang, Y. Jiang, J. Ma, H. Wu, D. Wacker, V. Katritch, G.W. Han, W. Liu, X. P. Huang, E. Vardy, J.D. McCorvy, X. Gao, X.E. Zhou, K. Melcher, C. Zhang, F. Bai, H. Yang, L. Yang, H. Jiang, B.L. Roth, V. Cherezov, R.C. Stevens, H.E. Xu, Structural basis for molecular recognition at serotonin receptors, Science 340 (80) (2013) 610–614, https://doi.org/10.1126/science.1232807.

[22] D. Wacker, C. Wang, V. Katritch, G.W. Han, X.P. Huang, E. Vardy, J.D. McCorvy, Y. Jiang, M. Chu, F.Y. Siu, W. Liu, H.E. Xu, V. Cherezov, B.L. Roth, R.C. Stevens, Structural features for functional selectivity at serotonin receptors, Science 340 (80) (2013) 615–619, https://doi.org/10.1126/science.1232808.

[23] D. Wacker, S. Wang, J.D. McCorvy, R.M. Betz, A.J. Venkatakrishnan, A. Levit, K. Lansu, Z.L. Schools, T. Che, D.E. Nichols, B.K. Shoichet, R.O. Dror, B.L. Roth, Crystal Structure of an LSD-Bound Human Serotonin Receptor, Cell 168 (2017) 377–389.e12, https://doi.org/10.1016/j.cell.2016.12.033.

[24] T. Passie, J.H. Halpern, D.O. Stichtenoth, H.M. Emrich, A. Hintzen, The pharmacology of lysergic acid diethylamide: A review, CNS Neurosci. Ther. 14 (2008) 295–314, https://doi.org/10.1111/j.1755-5949.2008.00059.x.
[25] Y. Peng, J.D. McCorvy, K. Harpsøe, K. Lansu, S. Yuan, P. Popov, L. Qu, M. Pu, T. Che, L.F. Nikolajsen, X.P. Huang, Y. Wu, L. Shen, W.E. Bjørn-Yoshimoto, K. Ding, D. Wacker, G.W. Han, J. Cheng, V. Katritch, A.A. Jensen, M.A. Hanson, S. Zhao, D. E. Gloriam, B.L. Roth, R.C. Stevens, Z.J. Liu, 5-HT2C Receptor Structures Reveal the Structural Basis of GPCR Polypharmacology, Cell 172 (2018) 719–730.e14, https://doi.org/10.1016/j.cell.2018.01.001.
[26] A.P. Bento, A. Gaulton, A. Hersey, L.J. Bellis, J. Chambers, M. Davies, F.A. Krüger, Y. Light, L. Mak, S. McGlinchey, M. Nowotka, G. Papadatos, R. Santos, J. P. Overington, The ChEMBL bioactivity database: An update, Nucleic Acids Res. 42 (2014) 1083–1090, https://doi.org/10.1093/nar/gkt1031.
[27] H. Liu, J.M. Farley, Effects of first and second generation antihistamines on muscarinic induced mucus gland cell ion transport, BMC Pharmacol. 5 (2005), https://doi.org/10.1186/1471-2210-5-8.
[28] T. Shimamura, M. Shiroishi, S. Weyand, H. Tsujimoto, G. Winter, V. Katritch, R. Abagyan, V. Cherezov, W. Liu, G.W. Han, T. Kobayashi, R.C. Stevens, S. Iwata, Structure of the human histamine H 1 receptor complex with doxepin, Nature 475 (2011) 65–70, https://doi.org/10.1038/nature10236.
[29] D.M. Thal, B. Sun, D. Feng, V. Nawaratne, K. Leach, C.C. Felder, M.G. Bures, D. A. Evans, W.I. Weis, P. Bachhawat, T.S. Kobilka, P.M. Sexton, B.K. Kobilka, A. Christopoulos, Crystal structures of the M1 and M4 muscarinic acetylcholine receptors, Nature 531 (2016) 335–340, https://doi.org/10.1038/nature17188.
[30] S.S. Auerbach, DrugMatrix in vitro pharmacology data, 2019. https://ntp.niehs.nih.gov/drugmatrix/index.html (accessed June 30, 2020).
[31] A.C. Kruse, J. Hu, A.C. Pan, D.H. Arlow, D.M. Rosenbaum, E. Rosemond, H. F. Green, T. Liu, P.S. Chae, R.O. Dror, D.E. Shaw, W.I. Weis, J. Wess, B.K. Kobilka, Structure and dynamics of the M3 muscarinic acetylcholine receptor, Nature 482 (2012) 552–556, https://doi.org/10.1038/nature10867.
[32] V. Isberg, C. de Graaf, A. Bortolato, V. Cherezov, V. Katritch, F.H. Marshall, S. Mordalski, J.-P. Pin, R.C. Stevens, G. Vriend, D.E. Gloriam, Generic GPCR residue numbers – Aligning topology maps while minding the gaps, Trends Pharmacol. Sci. 36 (2015) 22–31, https://doi.org/10.1016/j.tips.2014.11.001.
[33] J. Yin, K.Y.M. Chen, M.J. Clark, M. Hijazi, P. Kumari, X. Chen Bai, R.K. Sunahara, P. Barth, D.M. Rosenbaum, Structure of a D2 dopamine receptor–G-protein complex in a lipid membrane, Nature 584 (2020) 125–129, https://doi.org/10.1038/s41586-020-2379-5.
[34] D. Im, A. Inoue, T. Fujiwara, T. Nakane, Y. Yamanaka, T. Uemura, C. Mori, Y. Shiimura, K.T. Kimura, H. Asada, N. Nomura, T. Tanaka, A. Yamashita, E. Nango, K. Tono, F.M.N. Kadji, J. Aoki, S. Iwata, T. Shimamura, Structure of the dopamine D2 receptor in complex with the antipsychotic drug spiperone, Nat. Commun. 11 (2020) 1–11, https://doi.org/10.1038/s41467-020-20221-0.
[35] L. Fan, L. Tan, Z. Chen, J. Qi, F. Nie, Z. Luo, J. Cheng, S. Wang, Haloperidol bound D2 dopamine receptor structure inspired the discovery of subtype selective ligands, Nat. Commun. 11 (2020) 1074, https://doi.org/10.1038/s41467-020-14884-y.
[36] W. Liu, D. Wacker, C. Gati, G.W. Han, D. James, D. Wang, G. Nelson, U. Weierstall, V. Katritch, A. Barty, N.A. Zatsepin, D. Li, M. Messerschmidt, S. Boutet, G. J. Williams, J.E. Koglin, M.M. Seibert, C. Wang, S.T.A. Shah, S. Basu, R. Fromme, C. Kupitz, K.N. Rendek, I. Grotjohann, P. Fromme, R.A. Kirian, K.R. Beyerlein, T. A. White, H.N. Chapman, M. Caffrey, J.C.H. Spence, R.C. Stevens, V. Cherezov, Serial femtosecond crystallography of G protein-coupled receptors, Science 342 (80) (2013) 1521–1524, https://doi.org/10.1126/science.1244142.
[37] E.Y.T. Chien, W. Liu, Q. Zhao, V. Katritch, G.W. Han, M.A. Hanson, L. Shi, A. H. Newman, J.A. Javitch, V. Cherezov, R.C. Stevens, Structure of the human dopamine D3 receptor in complex with a D2/D3 selective antagonist, Science 330 (80) (2010) 1091–1095, https://doi.org/10.1126/science.1197410.
[38] A. Schrödinger Release 2013, Schrödinger, LLC, New York, NY, 2020, No Title, 2013.
[39] A. Schrödinger Release 2019-4, Schrödinger, LLC, New York, NY, 2020, No Title, 2019.
[40] C.P. Leslie, M. Biagetti, S. Bison, S.M. Bromidge, R. Di Fabio, D. Donati, A. Falchi, M.J. Garnier, A. Jaxa-Chamiec, G. Manchee, G. Merlo, D.A. Pizzi, L.P. Stasi, J. Tibasco, A. Vong, S.E. Ward, L. Zonzini, Discovery of 1-(3-{2-[4-(2-Methyl-5-quinolinyl)-1-piperazinyl]ethyl}phenyl) -2-imidazolidinone (GSK163090), a potent, selective, and orally active 5-HT 1A/B/D receptor antagonist, J. Med. Chem. 53 (2010) 8228–8240, https://doi.org/10.1021/jm100714c.
[41] A. Schrödinger Release 2017-4, Schrödinger, LLC, New York, NY, 2020, No Title, 2017.
[42] A. Calculator, version 5.1.4, ChemAxon Ltd: Budapest, Hungary, 2018-2020, ChemAxon Ltd: Budapest, Hungary, 2008.
[43] A. Corina, version 3.59, Molecular Networks GmbH, Germany and Altamira, LLC, USA, 2020, No Title, 2016.
[44] A. Molecular Operating Environment (MOE), version 2015.10, Chemical Computing Group ULC. 2020, No Title, 2016.
[45] O. Korb, T. Stützle, T.E. Exner, Empirical scoring functions for advanced Protein-Ligand docking with PLANTS, J. Chem. Inf. Model. 49 (2009) 84–96, https://doi.org/10.1021/ci800298z.
[46] G. Marcou, D. Rognan, Optimizing fragment and scaffold docking by use of molecular interaction fingerprints, J. Chem. Inf. Model. 47 (2007) 195–207, https://doi.org/10.1021/ci600342e.
[47] C. de Graaf, A.J. Kooistra, H.F. Vischer, V. Katritch, M. Kuijer, M. Shiroishi, S. Iwata, T. Shimamura, R.C. Stevens, I.J.P. de Esch, R. Leurs, Crystal structure-based virtual screening for fragment-like ligands of the human histamine H1 receptor, J. Med. Chem. 54 (2011) 8195–8206, https://doi.org/10.1021/jm2011589.
[48] https://www.maybridge.com/, 2016.
[49] Y. Zhang, A. Borrel, L. Ghemtio, L. Regad, G.B.A. Gennäs, A.C. Camproux, J. Yli-Kauhaluoma, H. Xhaard, Structural Isosteres of Phosphate Groups in the Protein Data Bank, J. Chem. Inf. Model. 57 (2017) 499–516, https://doi.org/10.1021/acs.jcim.6b00519.
[50] U. Le, B.J. Melancon, T.M. Bridges, P.N. Vinson, T.J. Utley, A. Lamsal, A. L. Rodriguez, D. Venable, D.J. Sheffler, C.K. Jones, A.L. Blobaum, M.R. Wood, J. S. Daniels, P.J. Conn, C.M. Niswender, C.W. Lindsley, C.R. Hopkins, Discovery of a selective M4 positive allosteric modulator based on the 3-amino-thieno[2,3-b] pyridine-2-carboxamide scaffold: Development of ML253, a potent and brain penetrant compound that is active in a preclinical model of schizophrenia, Bioorganic Med. Chem. Lett. 23 (2013) 346–350, https://doi.org/10.1016/j.bmcl.2012.10.073.
[51] G. Neudert, G. Klebe, fconv: Format conversion, manipulation and feature computation of molecular data, Bioinformatics 27 (2011) 1021–1022, https://doi.org/10.1093/bioinformatics/btr055.
[52] M. Kobeissi, O. Yazbeck, Y. Chreim, A convenient one-pot synthesis of polysubstituted pyrroles from N-protected succinimides, Tetrahedron Lett. 55 (2014) 2523–2526, https://doi.org/10.1016/j.tetlet.2014.03.021.
[53] W. Zhou, S. Li, W. Lu, J. Yuan, Y. Xu, H. Li, J. Huang, Z. Zhao, Isoindole-1,3-dione derivatives as RSK2 inhibitors: Synthesis, molecular docking simulation and SAR analysis, Medchemcomm. 7 (2016) 292–296, https://doi.org/10.1039/c5md00469a.
[54] Y.Y. Cheung, H. Yu, K. Xu, B. Zou, M. Wu, O.B. McManus, M. Li, C.W. Lindsley, C. R. Hopkins, Discovery of a series of 2-phenyl- N -(2-(pyrrolidin-1-yl)phenyl) acetamides as novel molecular switches that modulate modes of K v7.2 (KCNQ2) channel pharmacology: Identification of (S)-2-phenyl- N -(2-(pyrrolidin-1-yl) phenyl)butanamide (ML252) as a pote, J. Med. Chem. 55 (2012) 6975–6979, https://doi.org/10.1021/jm300700v.
[55] R. Bosma, R. Moritani, R. Leurs, H.F. Vischer, BRET-based β-arrestin2 recruitment to the histamine H1 receptor for investigating antihistamine binding kinetics, Elsevier, 2016, pp. 679–687.